

Tensegrity cell mechanical metamaterial with metal rubber

Qicheng Zhang,¹ Dayi Zhang,^{1,a)} Yousef Dobah,² Fabrizio Scarpa,^{2,a)} Fernando Fraternali,³ and Robert E. Skelton⁴

¹*School of Energy and Power Engineering, Beihang University, Beijing 100191, People's Republic of China*

²*Bristol Composites Institute (ACCIS), University of Bristol, University Walk, BS8 1TR Bristol, United Kingdom*

³*Department of Civil Engineering, University of Salerno, 84084 Fisciano, Italy*

⁴*Aerospace Engineering, Texas A&M, College Station, Texas 77843-3141, USA*

(Received 21 May 2018; accepted 7 July 2018; published online 20 July 2018)

We present here a design of the unit cell of a mechanical metamaterial based on the use of a tensegrity structural configuration with a metal rubber. Tensegrity combines the use of compression and tension-only elements, and allows the creation of structures with high rigidity per unit mass. Metal rubber is a multiscale porous metal material with high energy absorption and vibration damping capabilities under compressive load. The combination of the two structural and material concepts gives rise to a mechanical metamaterial with increased energy absorption and tuneable nonlinearity under quasi-static, vibration, and impact loading. We develop prototypes, models, and perform tests under static and dynamic loading conditions to assess the performance of this mechanical metamaterial. *Published by AIP Publishing.* <https://doi.org/10.1063/1.5040850>

Mechanical metamaterials (MM) have been recently ailed as a major paradigm to develop multiscale and multi-physics materials. Examples of recent mechanical metamaterial concepts are, for example, pentamodal lattices,^{1,2} periodic cellular configurations for energy absorption and harvesting³ (including topologies with random configurations^{4,5}), and configurations exhibiting both zero and negative materials characteristics.^{6,7} One of the main characteristics of MMs is their capability of hybridizing deformation mechanisms at multiple scale levels by coupling fields and properties from different physical domains. Examples of this coupling are magnetics within lattices to control negative stiffness⁷ and nonlinear wave propagation,⁸ piezoelectrics,^{9,10} shape memory polymers (SMPs),^{11,12} and cellular solids with unbounded thermal expansion properties.¹³ Metal rubbers (MRs) are a class of multiscale materials with unusual deformation properties. Metal rubber is a porous metal compound made from surface-treated helical wires, compressed in a mold. The base wire material can range from nickel¹⁴ to shape memory¹⁵ and soft magnetic alloys.¹⁶ Metal rubbers show loss factors under high-amplitude cyclic loadings between 12% and 26% that depend on their relative density, operational temperatures between 110 K and 650 K, and a strong strain hardening behavior that can be used to design high-performance vibration dampers. Metal rubber can be shaped and molded in different forms, also into assuming a negative Poisson's ratio behavior.¹⁷ Metal rubber inserts have been inserted as distributed dampers in an auxetic honeycomb platform, yielding modal damping ratios up to 45% in vibration transmissibility tests.¹⁸

A structural concept that has attracted significant interest within the metamaterials community is tensegrity.^{19,20} Tensegrity are spatially reticulated lightweight structures made from compressive bars and tendons with a highly

tuneable mechanical response that can range from hardening to softening, depending on the configuration adopted. In that sense, tensegrity systems can provide significant tuneable wave attenuation especially under nonlinear loading,²¹ which could also be used to control energy absorption under impact.²² Moreover, tensegrity is an excellent platform to embed smart or metamaterial capabilities, either with 3D-printed SMPs²³ or piezoelectric bars prisms.²⁴

In this letter, we present the design of a unit cell of a mechanical metamaterial made from a tensegrity T3 prism, with the compressive bars designed using metal rubber inserts. MR is a material with load-bearing capabilities under compression only; its high energy absorption capabilities coupled with the tuneable nonlinear compressive behavior of the tensegrity could provide unusual mechanical interactions at a global and local scale. We will show that the combined use of the MR material within the tensegrity configuration leads to high loss factors under cyclic quasi-static loading, increased damping properties in vibration environments, and augmented energy absorption under impact compared to the tensegrity prism alone.

The experimental set up incorporating the MR inserts into the tensegrity structure is shown in Fig. 1. Two separate aluminum bars are used to assemble the strut, with the MR specimen in the middle attached to the bars with metal glue. The MR is surrounded by an aluminum sleeve that increases the buckling stress of the strut and permits the metal rubber to deform axially. Each end of the strut includes steel joints, screws with an adjusting bolt and locking nuts; the latter are used to regulate the pre-tension in the string. The tensegrity has struts of 350 mm length and 20.5 mm of diameter, with horizontal string lengths of 225 mm and cross string lengths of 253.1 mm. The strings are made from steel (piano wire) of 0.61 mm diameter. The tension in the string is measured by an external microphone that detects the string first resonance, allowing one to calculate the related tensile force. Triangular plates terminate the tensegrity prism to allow for a uniform

^{a)} Authors to whom correspondence should be addressed: dayi@buaa.edu.cn and f.scarpa@bristol.ac.uk

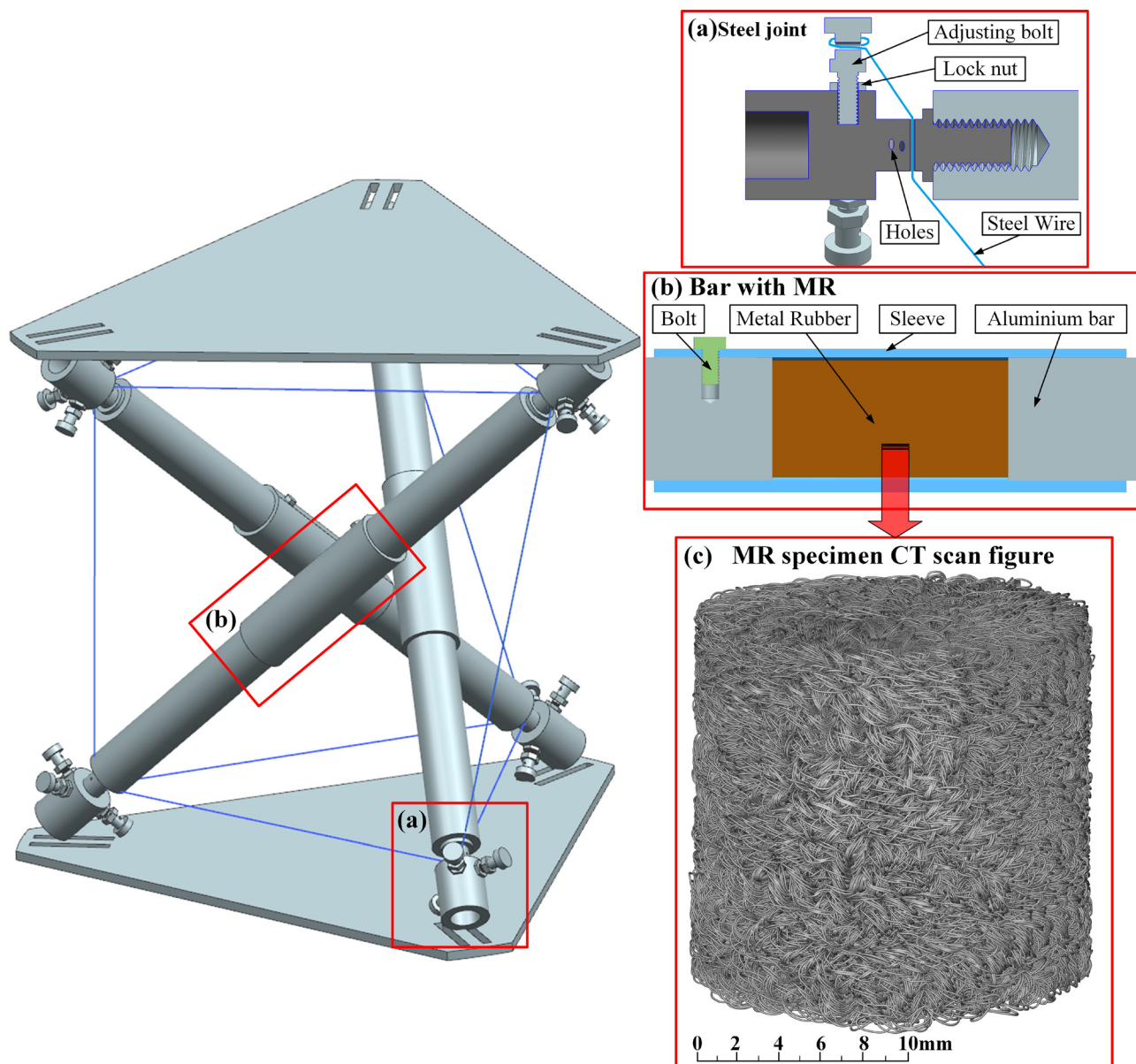


FIG. 1. Layout of the tensegrity mechanical metamaterial with the metal rubber.

distribution of the compressive load. MR samples of 20 mm diameter and 40 mm height are produced using nickel super-alloy helical wires of 0.12 mm diameter using the procedure outlined in Ref. 14. The samples have a 72% porosity, loss factors varying between 0.15 and 0.17 for pre-compression ranging from 63 kPa to 191 kPa, while the secant modulus varies between 1.3 MPa and 7.7 MPa.

The tensegrity prototypes (with and without MR) have been subjected to cyclic tests under force control at 1 N/s and triangular waveform (Shimatzu AG-X, 1 kN load cell). The initial stiffness of the tensegrity without MR is 67 N/mm (calculated up to a displacement of 0.2 mm), which then increases to 130 N/mm for a maximum displacement of 1.9 mm. The tensegrity with the metal rubber shows a remarkable $\sim 250\%$ increase in maximum compressive displacement, but a significantly lower stiffness (initially at 53 N/mm up to 0.2 mm, to then plateau at 32 N/mm after 1.5 mm). To understand why the addition of the metal rubber provides this particular behavior, we have developed a model

from the theoretical framework proposed in Ref. 25 (details in the [supplementary material](#)). The design of the joints involves the existence of an additional rotational stiffness that is not present in classical tensegrity models. Moreover, the friction existing in the tensegrities here involves contributions from the sleeves, joints, and compression plates from the rig. The overall tensegrity friction force has not the simple global stick-slip effect that depends only on the overall compressive force.²⁶ The model shows that the equivalent angular stiffness of the MR tensegrity is significantly lower than the one of the pristine case, and this leads to a larger stroke under compression with more energy dissipated by friction (Fig. 2). On the contrary, the joints of the pristine tensegrity remain in stick conditions during the loading, and less displacement and dissipated energy are produced. The good agreement between models and experimental results corroborates these findings. The loss factor of the pristine tensegrity is 0.127, which indicates the level of internal equivalent damping within the system. Compounded by the

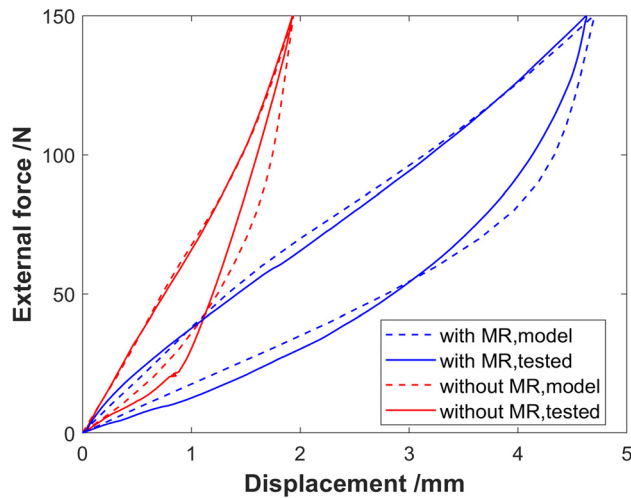


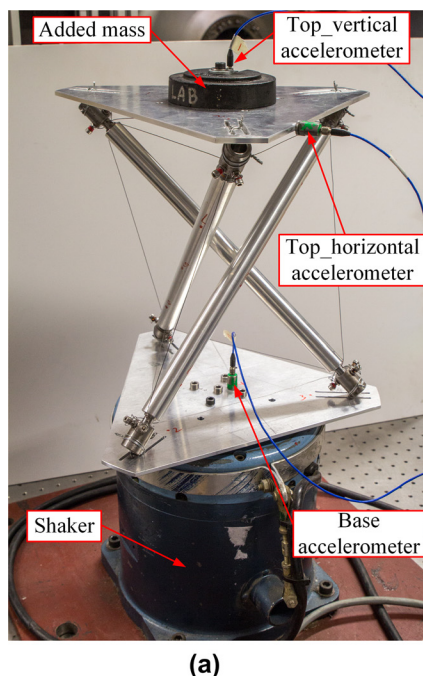
FIG. 2. Comparison between experimental and model quasi-static cyclic compressive loading for the tensegrity metamaterials.

large increase in compressive stroke, the presence of the metal rubber inserts also provides a significant 30% augmentation of the dissipated energy.

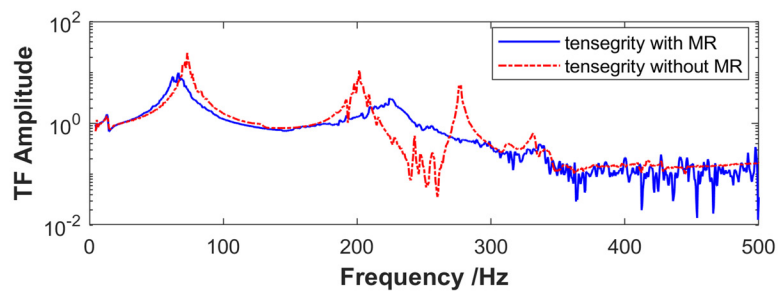
We have then performed vibration transmissibility tests [Fig. 3(a)] using white noise, and impact hammering for modal analysis (for details see [supplementary material](#)). The natural frequencies of the tensegrity without MR vary between 20 Hz and 332 Hz. Sine sweep tests at 10 Hz, 30 Hz, and 180 Hz indicate that the 1st mode is a twisting one and the second mode (at 70 Hz) is dilatational along the vertical direction. The Bode plot of the transmissibility (ratio of accelerations between the top and bottom plate) also indicates the presence of another global extensional mode at 200 Hz [Fig. 3(b)] (see [supplementary material](#)). A series of localized modes related to the strings resonances are distributed within the 180 Hz–250 Hz, and these produce global

modes in the tensegrity which are difficult to associate to a specific single deformation mode.²⁷ The Bode plot of the white noise excitation [Figs. 3(a) and 3(c)] shows a clear distinction between the tensegrity with the metal rubber and without. While the first and second natural frequencies are virtually unchanged by the presence of the MR inserts (although the dilatational mode of the MR tensegrity is almost 3 dB lower than the one of the pristine prism), the metal rubber configuration shows both a stiffening (i.e., increase in the natural frequency by 22 Hz) and a very remarkable 7 dB attenuation of the transmissibility compared to the non-MR tensegrity. The MR also contributes to dissipate energy and stabilize the response of the tensegrity up to 330 Hz. The reason behind the stiffening and dampening effect is its increasing equivalent storage modulus (3–7 MPa) for frequencies above 150 Hz of the MR and loss factors all above 15%.²⁸

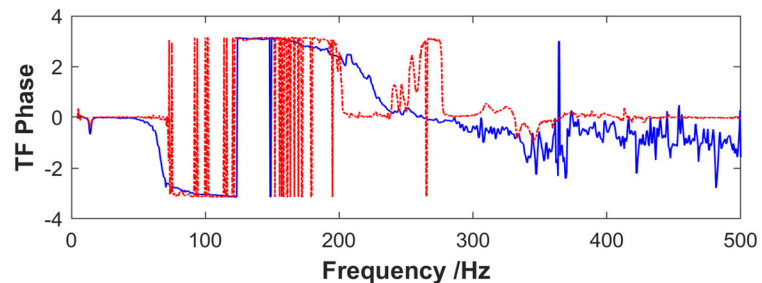
We have evaluated the impact properties of our tensegrity systems using a drop tower facility [CEAST 9340 Instron, UK; Fig. 4(a)]. The tests have been carried out at a kinetic energy level of 2.5 J (drop weight 6.87 kg, height 37.2 mm, and sampling frequency 273 kHz). The behavior of the two tensegrity systems in terms of energy absorbed is quite different. While the tensegrity without MR tends to rise, peak, and plateau relatively fast, the presence of the MR in the first 20 ms leads to lower energy absorbed initially, followed by higher values of energy [Fig. 4(b)]. The spectrum of the reaction load is also quite different. The two tensegrities have the loads spread within the ~0–150 Hz and ~350 Hz–600 Hz bands, with the latter bandwidth corresponding to modes of the plate. The first band corresponds to the global twisting and extensional modes observed from the modal analysis. While the magnitude of the loads in the second frequency band shows negligible differences between the two configurations, it is quite clear that the MR tensegrity



(a)



(b)



(c)

FIG. 3. (a) Vibration transmissibility rig with tensegrity specimen; Bode plot for the transmissibility magnitude (a) and phase (b) with a base r.m.s. acceleration of 0.7 g.

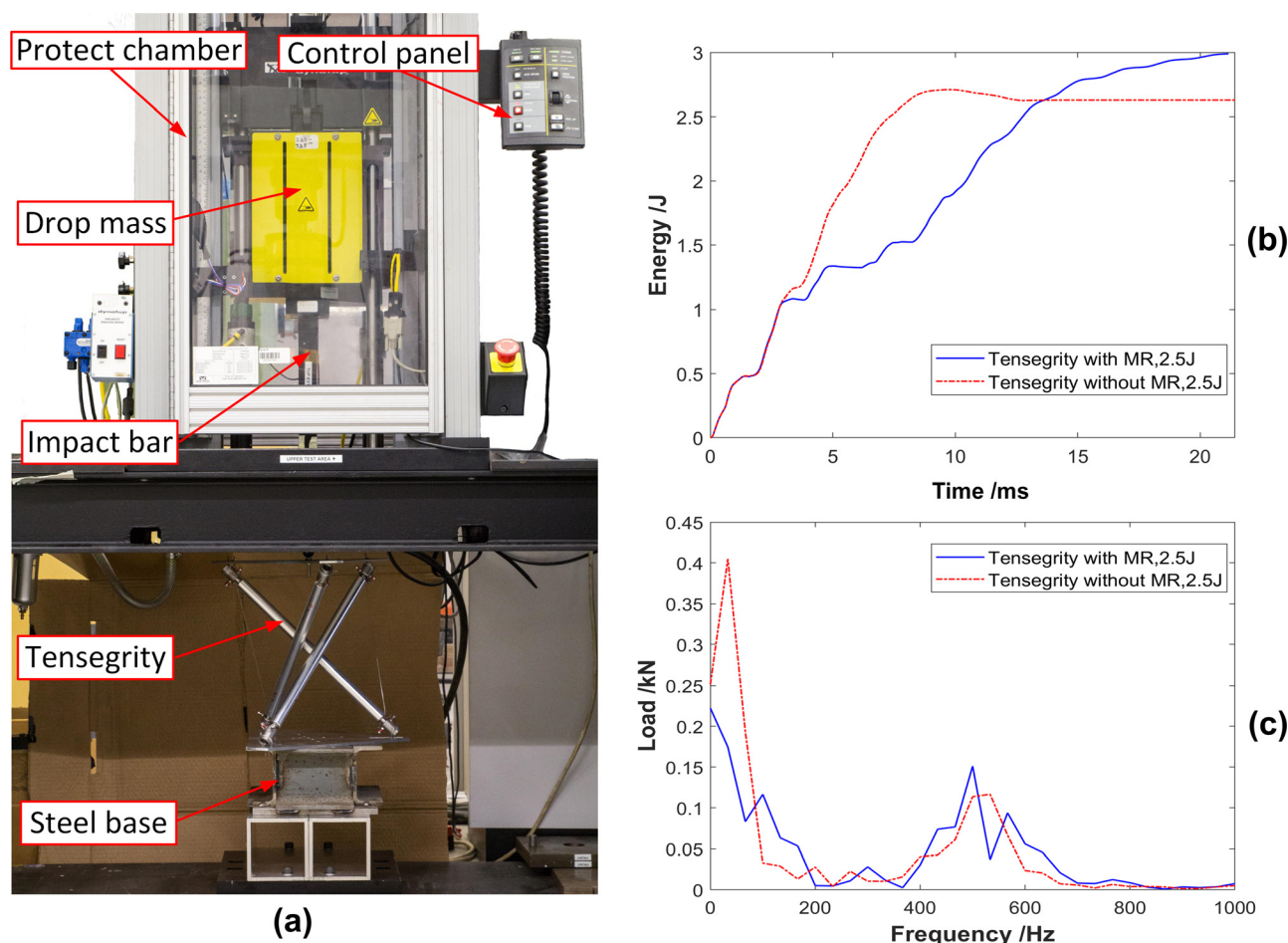


FIG. 4. (a) Drop tower test rig with a MR tensegrity specimen. The tensegrity is placed on a steel base and exposed to the drop mass in a protect chamber. The test is controlled through the right panel. (b) Energy absorbed vs. time and (c) load spectrum of the impacts for the tensegrity with and without MR.

provides a significant $\sim 50\%$ reduction of the maximum impact load in the lowest spectrum band.

In summary, the tensegrity mechanical metamaterial with metal rubber shows enhanced compliance and remarkable energy absorption under quasi-static, dynamic, and impact loading conditions. The concept here proposed gives also evidence of the versatility and promise to use tensegrity paradigms to produce different classes of mechanical metamaterials. The enhanced damping capacity of tensegrity units enriched by MR elements—as compared to standard tensegrity—may lead to increase the engineering potential of tensegrity metamaterials that perform impact protection through the coupling of solitary wave dynamics²¹ and energy absorption.

See [supplementary material](#) for the model describing the tensegrity prism with the metal rubber inserts has been developed by adding the additional torsional springs and a sigmoid friction force related to the loading and unloading cycles to the original framework described in Ref. 25 The experimental modal analysis and vibration transmissibility have been performed using impact hammers, electrodynamic shakers and accelerometers at controlled base excitation levels. More details can be found in the [supplementary material](#).

F.S. and R.E.S. thank the UK Royal Society Grant No. IE161769 for the funding of the International Collaboration

Scheme between Bristol and Texas A&M. Q.Z. and D.Z. acknowledge the National Natural Science Foundation of China (Grant Nos. 51475021 and 11672017) and the China Scholarship Council for the financial support during their stay in Bristol. F.F. acknowledges financial support from the Italian Ministry of Education, University and Research (MIUR) under the “Departments of Excellence” Grant No. L.232/2016.

¹M. Kadic, T. Bückmann, N. Stenger, M. Thiel, and M. Wegener, *Appl. Phys. Lett.* **100**(19), 191901 (2012).

²R. Hedayati, A. M. Leeflang, and A. A. Zadpoor, *Appl. Phys. Lett.* **110**(9), 091905 (2017).

³Y. Li, E. Baker, T. Reissman, C. Sun, and W. K. Liu, *Appl. Phys. Lett.* **111**(25), 251903 (2017).

⁴N. Grima Joseph, M. Luke, M. Azzopardi Keith, and G. Ruben, *Adv. Mater.* **28**(2), 385 (2016).

⁵M. J. Mirzaali, R. Hedayati, P. Vena, L. Vergani, M. Strano, and A. A. Zadpoor, *Appl. Phys. Lett.* **111**(5), 051903 (2017).

⁶X. Wang, X. Luo, H. Zhao, and Z. Huang, *Appl. Phys. Lett.* **112**(2), 021901 (2018).

⁷A. M. Hewage Trishan, L. Alderson Kim, A. Andrew, and S. Fabrizio, *Adv. Mater.* **28**(46), 10116 (2016).

⁸M. Schaeffer and M. Ruzzene, *J. Appl. Phys.* **117**(19), 194903 (2015).

⁹O. Acher, M. Ledieu, A. Bardaine, and F. Levassort, *Appl. Phys. Lett.* **93**(3), 032501 (2008).

¹⁰X. Zhang, D. Wu, C. Sun, and X. Zhang, *Phys. Rev. B* **76**(8), 085318 (2007).

¹¹K. Boba, M. Bianchi, G. McCombe, R. Gatt, A. C. Griffin, R. M. Richardson, F. Scarpa, I. Hamerton, and J. N. Grima, *ACS Appl. Mater. Interfaces* **8**(31), 20319 (2016).

¹²M. J. Mirzaali, S. Janbaz, M. Strano, L. Vergani, and A. A. Zadpoor, *Sci. Rep.* **8**(1), 965 (2018).

- ¹³R. Lakes, *Appl. Phys. Lett.* **90**(22), 221905 (2007).
- ¹⁴D. Zhang, F. Scarpa, Y. Ma, K. Boba, J. Hong, and H. Lu, *Mater. Sci. Eng.: A* **580**, 305 (2013).
- ¹⁵Y. Ma, Q. Zhang, D. Zhang, F. Scarpa, B. Liu, and J. Hong, *Acta Mater.* **96**, 89 (2015).
- ¹⁶M. Yanhong, H. Wenzhong, Z. Dayi, Z. Qicheng, and H. Jie, *Smart Mater. Struct.* **25**(9), 095015 (2016).
- ¹⁷H. Guo, T. Qingbiao, J. Guofeng, and L. Qiuyan, *Smart Mater. Struct.* **23**(9), 095011 (2014).
- ¹⁸M. Yanhong, S. Fabrizio, Z. Dayi, Z. Bin, C. Lulu, and H. Jie, *Smart Mater. Struct.* **22**(8), 084012 (2013).
- ¹⁹K. D. Snelson, U.S. patent 3,169,611 (1 Feb 1965).
- ²⁰R. E. Skelton and M. C. D. Oliveira, *Tensegrity Systems* (Springer, Berlin, 2011).
- ²¹F. Fraternali, G. Carpentieri, A. Amendola, R. E. Skelton, and V. F. Nesterenko, *Appl. Phys. Lett.* **105**(20), 201903 (2014).
- ²²V. SunSpiral, G. Gorospe, J. Bruce, A. Iscen, G. Korbel, S. Milam, A. Agogino, and D. Atkinson, *Int. J. Planet. Probes* **7** (2013).
- ²³K. Liu, J. Wu, G. H. Paulino, and H. J. Qi, *Sci. Rep.* **7**(1), 3511 (2017).
- ²⁴D. P. Williams, W. B. Carlson, W. A. Schulze, and S. M. Pilgrim, *Mater. Res. Innovations* **3**(4), 226 (2000).
- ²⁵F. Fraternali, G. Carpentieri, and A. Amendola, *J. Mech. Phys. Solids* **74**, 136 (2015).
- ²⁶D. Zhang, Y. Xia, F. Scarpa, J. Hong, and Y. Ma, *Sci. Rep.* **7**, 12874 (2017).
- ²⁷N. B. H. Ali and I. F. C. Smith, *Int. J. Solids Struct.* **47**, 1285 (2010).
- ²⁸D. Zhang, F. Scarpa, Y. Ma, J. Hong, and Y. Mahadik, *Mater. Des.* (1980-2015) **56**, 69 (2014).